The GATOR2–mTORC2 axis mediates Sestrin2-induced AKT Ser/Thr kinase activation

Allison Ho Kowalsky[‡1], Sim Namkoong[‡§1], [ORCID] Eric Mettetal[‡], Hwan-Woo Park[‡¶], [ORCID] Dubek Kazyken[‖], Diane C. Fingar[‖], and [ORCID] Jun Hee Lee[‡2]

From the Departments of ‡Molecular & Integrative Physiology and ‖Cell & Developmental Biology, University of Michigan Medical School, Ann Arbor, Michigan 48109, the §Department of Biochemistry, College of Natural Sciences, Kangwon National University, Chuncheon, Gangwon 24341, Republic of Korea, and the ¶Department of Cell Biology, Myunggok Medical Research Institute, Konyang University College of Medicine, Daejeon 35365, Republic of Korea

Edited by Alex Toker

Sestrins represent a family of stress-inducible proteins that prevent the progression of many age- and obesity-associated disorders. Endogenous Sestrins maintain insulin-dependent AKT Ser/Thr kinase (AKT) activation during high-fat diet–induced obesity, and overexpressed Sestrins activate AKT in various cell types, including liver and skeletal muscle cells. Although Sestrin-mediated AKT activation improves metabolic parameters, the mechanistic details underlying such improvement remain elusive. Here, we investigated how Sestrin2, the Sestrin homolog highly expressed in liver, induces strong AKT activation. We found that two known targets of Sestrin2, mTOR complex (mTORC) 1 and AMP-activated protein kinase, are not required for Sestrin2-induced AKT activation. Rather, phosphoinositol 3-kinase and mTORC2, kinases upstream of AKT, were essential for Sestrin2-induced AKT activation. Among these kinases, mTORC2 catalytic activity was strongly up-regulated upon Sestrin2 overexpression in an *in vitro* kinase assay, indicating that mTORC2 may represent the major link between Sestrin2 and AKT. As reported previously, Sestrin2 interacted with mTORC2; however, we found here that this interaction occurs indirectly through GATOR2, a pentameric protein complex that directly interacts with Sestrin2. Deleting or silencing WDR24 (WD repeat domain 24), the GATOR2 component essential for the Sestrin2–GATOR2 interaction, or WDR59, the GATOR2 component essential for the GATOR2–mTORC2 interaction, completely ablated Sestrin2-induced AKT activation. We also noted that Sestrin2 also directly binds to the pleckstrin homology domain of AKT and induces AKT translocation to the plasma membrane. These results uncover a signaling mechanism whereby Sestrin2 activates AKT through GATOR2 and mTORC2.

Sestrins are highly conserved, stress-induced proteins with antiaging properties in model organisms such as worms and flies [1, 2]. In the mammalian genome, three Sestrin paralogs (Sestrin1–3) exist [3]. Sestrin proteins have two important functions: reducing reactive oxygen species [4, 5] and inhibiting mTOR complex 1 (mTORC1)[3] [1, 6]. Many studies have also shown that Sestrin2 is important for metabolic homeostasis, especially during nutritional overload. For example, Sestrin2 was required to maintain insulin sensitivity in the liver upon high-fat diet (HFD)–induced dietary obesity and *Lep^{ob}* mutation-induced genetic obesity [7]. Under lipotoxic conditions, Sestrin2 was selectively up-regulated in the liver to alleviate endoplasmic reticulum (ER) stress by inhibiting mTORC1, thereby attenuating the development of steatohepatitis [8]. Likewise, Sestrin3, another Sestrin paralog, is also expressed in the liver and up-regulates the insulin-AKT signaling pathway during HFD and obesity [9]. These metabolic studies revealed that, in addition to oxidative stress reduction and mTORC1 down-regulation, Sestrins also up-regulate AKT signaling [7, 9]. Sestrin-induced AKT activation was also observed in *Drosophila* [7].

The molecular structure of Sestrin2 revealed a structural basis for Sestrin2's formerly characterized biochemical functions [5, 10]. A helix–turn–helix motif, composed of a proton relay system and reactive Cys-125, mediates the oxidoreductase function of Sestrin2 in reducing alkylhydroperoxides [5]. The DD motif, composed of two adjacent Asp-406 and Asp-407 residues in a loop, was important for the interaction between Sestrin2 and GATOR2, a pentameric protein complex regulat-

[3] The abbreviations used are: mTORC, mTOR complex; HFD, high-fat diet; AMPK, AMP-activated protein kinase; PI3K, phosphoinositol 3-kinase; PH, pleckstrin homology; PDK, phosphoinositide-dependent kinase; Ad-GFP, adenovirus(es) expressing GFP; Ad-SESN2, adenovirus(es) expressing Sestrin2; PA, palmitic acid; ITT, insulin tolerance test; DMEM, Dulbecco's modified Eagle's medium; HA, hemagglutinin; MEF, mouse embryonic fibroblast.

ing mTORC1 signaling (5, 10). Mutation in either of these two Asp residues nullifies Sestrin2's ability to down-regulate mTORC1 (5). Through the DD motif, Sestrin2 directly interacts with GATOR2 and releases it from inhibiting GATOR1, a trimeric protein complex with GTPase activity on the mTORC1-activating Rag proteins (5, 11–13). Therefore, Sestrin2 inhibits mTORC1 by inhibiting GATOR2 and allowing GATOR1 to inhibit the Rag proteins (11–13). Although the detailed mechanism is yet to be elucidated, the Sestrin2–GATOR2 interaction was also critical for AMPK activation (5), which is also critical for Sestrin2-mediated mTORC1 down-regulation in many different cell types and physiological contexts (1, 6, 14–18). Therefore, it is possible that GATOR2 has functions outside of mTORC1 regulation, mediating Sestrin2 output to other effector molecules and target pathways. GATOR2 consists of five proteins: WDR24, WDR59, MIOS, SEH1L, and SEC13 (19). Among these components, WDR24 and SEH1L are critical for physically interacting with Sestrin2 (12).

AKT is a major regulatory protein downstream of the insulin receptor that is responsible for many glucose- and lipid-regulating functions (20). Upon insulin stimulation, AKT is activated and phosphorylates a wide range of protein substrates to inhibit gluconeogenesis and up-regulate glycogenesis and lipogenesis. In addition to its metabolic regulation, AKT also promotes cell growth and proliferation and is implicated in many cancers. AKT has two active phosphorylation sites, Thr-308 and Ser-473, which are phosphorylated by phosphoinositide-dependent kinase 1 (PDK1) and mTORC2, respectively. Upon activation of the insulin signaling cascade leading to phosphoinositol 3-kinase (PI3K) activation, a second messenger, phosphatidylinositol 3,4,5-triphosphate, accumulates in the plasma membrane, which recruits PDK1, mTORC2, and AKT and induces PDK1 and mTORC2 to phosphorylate and activate AKT (20).

Sestrin-induced AKT activation was observed in a variety of cellular and physiological contexts, in addition to the insulin resistance and obesity contexts (7, 9). For instance, Sestrins have been shown to positively regulate AKT in cancer cells to protect against environmental stress, such as UV irradiation, energetic stress, and chemical stress (21–25). Sestrins are also important for muscle AKT activation, and the Sestrin-dependent AKT regulation is critical for producing exercise benefits and preventing age- and disuse-associated atrophy (26, 27). There have been several mechanisms proposed to explain Sestrin-induced AKT activation. The first is that Sestrin-induced mTORC1 inhibition releases the insulin receptor signaling pathway from mTORC1/S6K-mediated negative feedback inhibition (28). In this model, chronic mTORC1 activation induces S6K-dependent insulin receptor substrate serine phosphorylation, which attenuates signal transduction from the insulin receptor to PI3K (29). Therefore, Sestrin-mediated mTORC1 inhibition can indirectly up-regulate PI3K-AKT signaling (28). Consistent with this model, loss of Sestrin2 up-regulated S6K-mediated inhibitory serine phosphorylation of insulin receptor substrate while down-regulating insulin receptor-mediated activatory tyrosine phosphorylation (7). In addition to the S6K-mediated feedback, Sestrin may also down-regulate additional pathways that lead to insulin resistance,

such as ER stress (8) and inflammation pathways (30). Furthermore, several recent studies also suggested that Sestrin-dependent AKT activation could be independent of mTORC1 and directly through mTORC2 (9, 23). Still, the mechanistic details of how Sestrin2 regulates AKT remain incompletely understood.

In this study, we investigated the molecular mechanism by which Sestrin2 induces AKT activation in liver cells. We found that GATOR2 and mTORC2 link Sestrin2 to AKT activation. This new mechanism explains, at least in part, how Sestrin2 promotes metabolic homeostasis through increased AKT activity.

Results

Sestrin2 overexpression improves glucose and lipid regulation in HFD mice

Extensive studies have established that endogenous Sestrins protect against obesity-associated fatty liver and insulin resistance (7–9, 28). Based on these findings, we tested whether Sestrin2 overexpression could improve metabolic regulation in obese WT mice under HFD conditions. For this, adenoviruses expressing GFP (Ad-GFP) or Sestrin2 (Ad-SESN2) were administered to weight and age-matched mice through tail vein injections. Strikingly, after adenoviral expression of Sestrin2, both basal and insulin-reduced blood glucose levels were strongly decreased (Fig. 1A), and HFD-induced lipid accumulation in the liver tissue was also strongly decreased (Fig. 1B). Nevertheless, Ad-SESN2 transduction did not substantially change overall body weight (Fig. 1C). Consistent with reduction in blood glucose (Fig. 1A) and liver fat levels (Fig. 1B), mRNA expression of gluconeogenic and lipogenic genes were strongly decreased by Sestrin2 overexpression (Fig. 1D). Therefore, the evidence suggests that Sestrin2 overexpression in liver was sufficient to alter hepatic transcription of metabolic genes and subsequently restore glucose and lipid homeostasis in obese, insulin-resistant mice.

Sestrin2 overexpression induces strong AKT activation in mouse liver and HepG2 cells

Upon examining liver lysates obtained from HFD-fed mice, we found that overexpression of Sestrin2 increased AKT phosphorylation on both the PDK1-mediated activation loop site (Thr-308) and the mTORC2-mediated hydrophobic motif site (Ser-473) relative to control livers, indicating strong AKT activation. In fact, Sestrin2 increased phosphorylation on these sites to a level higher than that mediated by acute insulin treatment of control mice (Fig. 2A). Moreover, Sestrin2 overexpression increased basal liver AKT phosphorylation strongly in HFD-fed mice (Fig. 2A) and consistently increased AKT phosphorylation in HepG2 cells (Fig. 2B). However, unlike in the liver, where the effect of Sestrin2 on AKT phosphorylation was stronger than insulin (Fig. 2A), the effects of Sestrin2 and insulin on AKT phosphorylation were additive in HepG2 cells (Fig. 2B). Sestrin2 overexpression also rescued AKT phosphorylation in the presence of inhibitory palmitic acid (PA) treatment, a saturated fatty acid that produces strong cellular insulin resistance (31) (Fig. 2, B and C). Conversely, silencing Sestrin2 in HepG2 cells decreased AKT phosphorylation in both normal and PA-treated conditions (Fig. 2C).
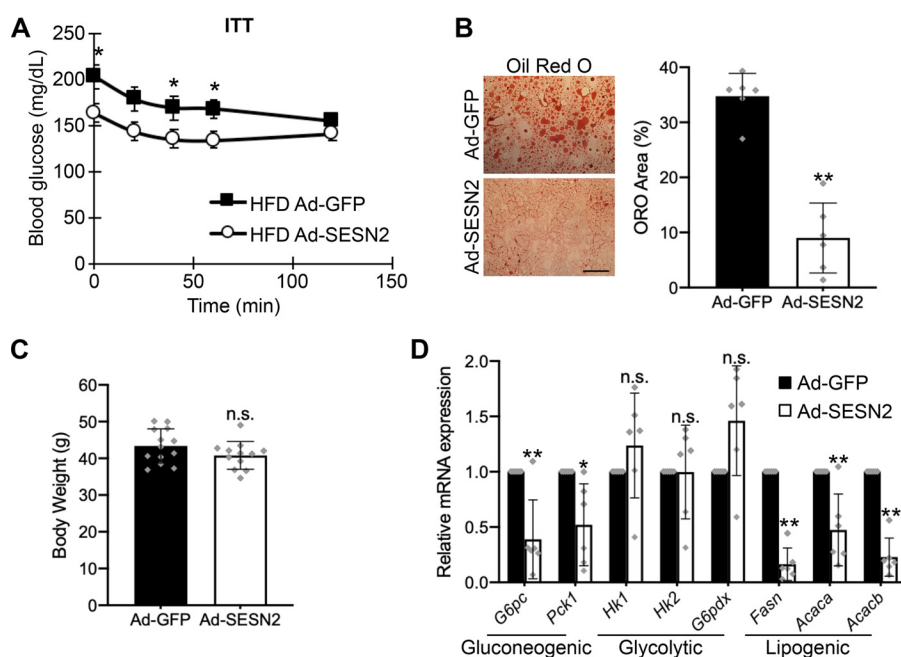
Figure 1. Sestrin2 overexpression improves glucose and lipid homeostasis in HFD mice. 2-month-old C57BL/6J mice were fed a HFD for at least 2 additional months. The mice were then administered tail vein injections of adenoviruses (10^9 pfu) that express GFP (Ad-GFP; $n = 13$) or Sestrin2 (Ad-SESN2; $n = 12$). *A*, 4–10 days after adenovirus administration, the mice were fasted for 6 h and then subjected to ITTs (0.65 unit/kg). *B*, fresh frozen liver sections were stained with Oil Red O (*ORO*) and quantified ($n = 6$) to determine fat accumulation in liver tissue. *Scale bar*, 200 μm. *C*, body weights of animals at 10 days after adenovirus administration. *D*, liver lysates were analyzed by quantitative RT-PCR to examine expression of metabolism-regulating genes in the liver tissue ($n = 6$). The data are presented as means ± S.D. with individual data points (*bar graphs*) or means ± S.E. (*line graphs*). The p values were calculated between Ad-GFP and Ad-SESN2 groups from a two-tailed Student's t test: *, $p < 0.05$; **, $p < 0.01$.
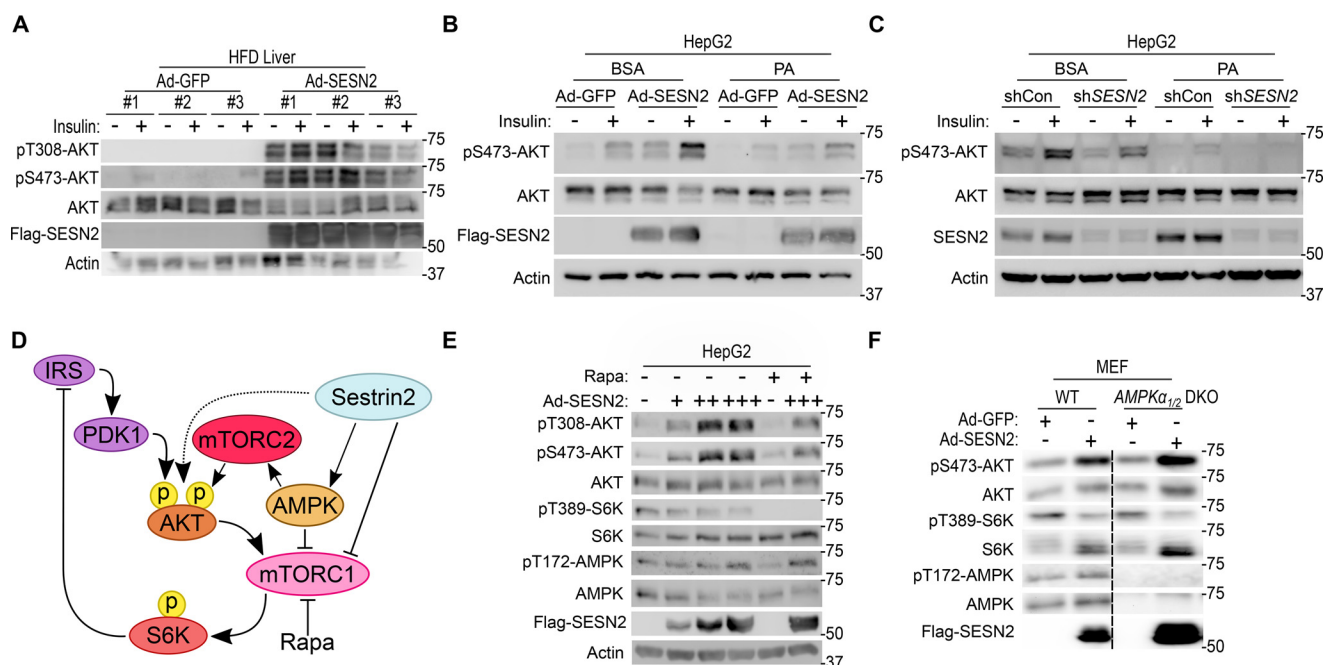

Figure 2. Sestrin2 activates AKT independently of mTORC1 and AMPK. *A*, at 10 days after Ad-GFP or Ad-SESN2 administration, mouse livers were collected before (−) and 10 min after (+) an injection of insulin (0.8 unit/kg). Liver lysates were analyzed by immunoblotting. *B* and *C*, HepG2 cells were treated with BSA loaded with PA (500 μM) for 9 h and then treated with insulin (+, 50 nmol) for 20 min. BSA-only and water-only (−) samples were used as controls. *B*, HepG2 cells were acutely infected with control or Sestrin2-overexpressing adenoviruses before BSA and PA treatments. *C*, HepG2 cells were stably infected with control (shRNA–Luciferase) and shRNA-SESN2 lentiviruses before BSA and PA treatments. All samples were analyzed by immunoblotting. *D*, schematic of potential molecular mechanisms that can account for Sestrin2-induced AKT activation. *E*, HepG2 cells were infected with Ad-GFP or Ad-SESN2 for 12 h, serum-starved with or without rapamycin (*Rapa*, 10 nM) for 24 h, and subjected to immunoblotting. *F*, WT and $Ampk\alpha_1^{-/-}/Ampk\alpha_2^{-/-}$ MEFs were serum-starved in DMEM with 0.1% FBS, treated with Ad-GFP or Ad-SESN2 overnight, and then analyzed by immunoblotting.
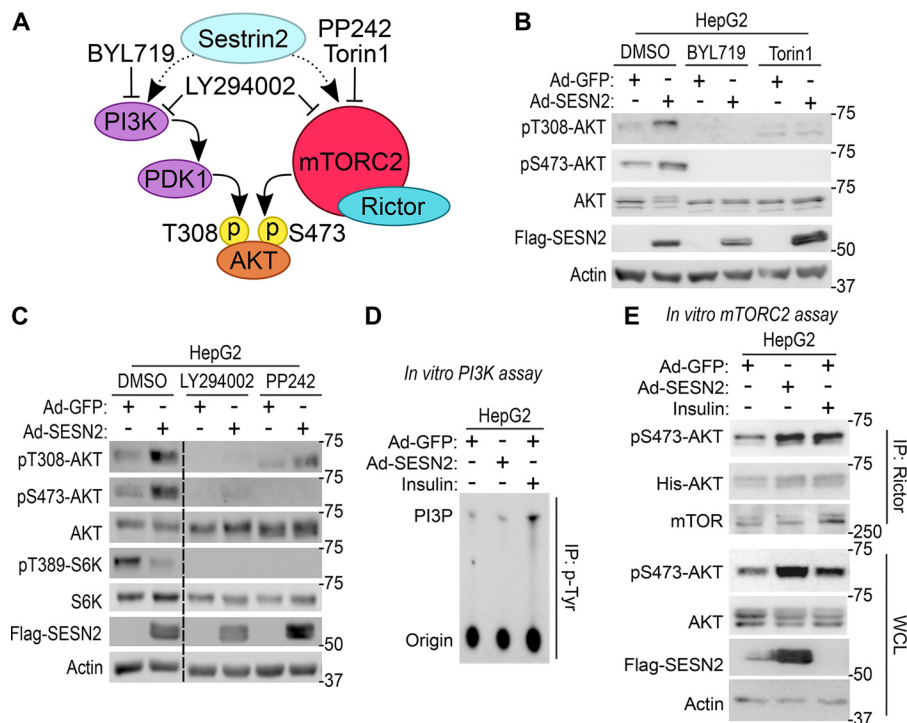
Figure 3. Sestrin2 up-regulates mTORC2. *A*, schematic of AKT-regulating pathways and drugs targeting the pathway. *B* and *C*, HepG2 cells were treated with Ad-GFP or Ad-SESN2; serum-starved; treated with DMSO (control), BYL719 (10 nM), Torin1 (200 nM), LY294002 (20 μM), or PP242 (5 μM); and then analyzed by immunoblotting. *D* and *E*, HepG2 cells infected with Ad-GFP or Ad-SESN2 were stimulated with or without insulin (100 nM). *D*, lysates were subjected to p-Tyr immunoprecipitation (*IP*), subjected to a lipid kinase assay with [γ-^{32}P]ATP and phosphatidylinositol, and then subjected to TLC and autoradiography to visualize radiolabeled PI3P. *E*, lysates were subjected to anti-Rictor immunoprecipitation, and subjected to an *in vitro* kinase assay using ATP and recombinant full-length inactive His-AKT. The reaction mixtures, as well as original whole cell lysates (*WCL*), were subjected to subsequent immunoblot analyses for examining protein amounts and phosphorylation.

Sestrin2 overexpression up-regulates AKT independently of mTORC1 and AMPK

Because Sestrin2 inhibits mTORC1 and thus suppresses mTORC1/S6K1-mediated negative feedback on insulin signaling and PI3K flux, it was possible that Sestrin2 activates AKT indirectly through this negative feedback mechanism (29) (Fig. 2D). To test whether mTORC1 inhibition mediates Sestrin2-induced AKT activation, we transduced HepG2 cells with increasing dosages of Sestrin2 and co-treated the cells with rapamycin, an mTORC1-specific inhibitor. As expected, Sestrin2 dose-dependently activated AKT in HepG2 cells (Fig. 2E). Interestingly, Sestrin2-induced AKT activation was still observed in rapamycin-treated cells, in which mTORC1-dependent S6K1 phosphorylation was completely blocked (Fig. 2E), indicating that Sestrin2 activates AKT independently of the mTORC1/S6K1-mediated negative feedback loop (Fig. 2D). More recently, it was reported that AMPK promotes mTORC2 signaling in response to acute energetic stress through phosphorylation of mTOR and mTORC2 partner proteins (32). Because Sestrin2 activates AMPK, it was possible that Sestrin2 increases mTORC2-mediated AKT phosphorylation and activation through AMPK (Fig. 2D). To determine whether Sestrin2-induced AKT activation was occurring through AMPK, we treated WT and *Ampk*-null mouse embryonic fibroblasts (WT and *Ampkα₁⁻/⁻/Ampkα₂⁻/⁻* DKO MEFs) with Ad-SESN2. As observed in HepG2 cells, Sestrin2 still activated AKT in both WT and *Ampkα₁/₂* DKO MEFs, indicating that this regulation was independent of AMPK (Fig. 2F). These results

reveal a novel mechanism by which Sestrin2 induces AKT activation independently of mTORC1 and AMPK, two established effectors of Sestrin2.

PI3K and mTORC2 are required for Sestrin2-induced AKT activation

To further investigate the mechanism by which Sestrin2 activates AKT, we treated HepG2 cells with a panel of chemical inhibitors specific for signaling components that regulate AKT (Fig. 3A). BYL719, a PI3K-specific inhibitor, and Torin1, an active site mTOR inhibitor (inhibits both mTORC1 and mTORC2), completely ablated Sestrin2-induced AKT activation (Fig. 3B), indicating that both PI3K and mTOR, specifically mTORC2, are required for Sestrin2-induced AKT activation. Consistent with this, LY294002, an inhibitor of both PI3K and mTOR, and PP242, another active site mTOR inhibitor, also blocked Sestrin2-induced AKT activation (Fig. 3C). Therefore, these data suggest that both PI3K and mTORC2 activities are required for Sestrin2-induced AKT activation.

Sestrin2 up-regulates the catalytic activity of mTORC2 but not PI3K

Because both PI3K and mTORC2 were required for Sestrin2-induced AKT activation, we assessed the effect of Sestrin2 on these signaling components through *in vitro* kinase assays. Although the established PI3K activator insulin was able to prominently increase the lipid kinase activity of PI3K, Sestrin2 did not have a measurable effect on PI3K activity in basal
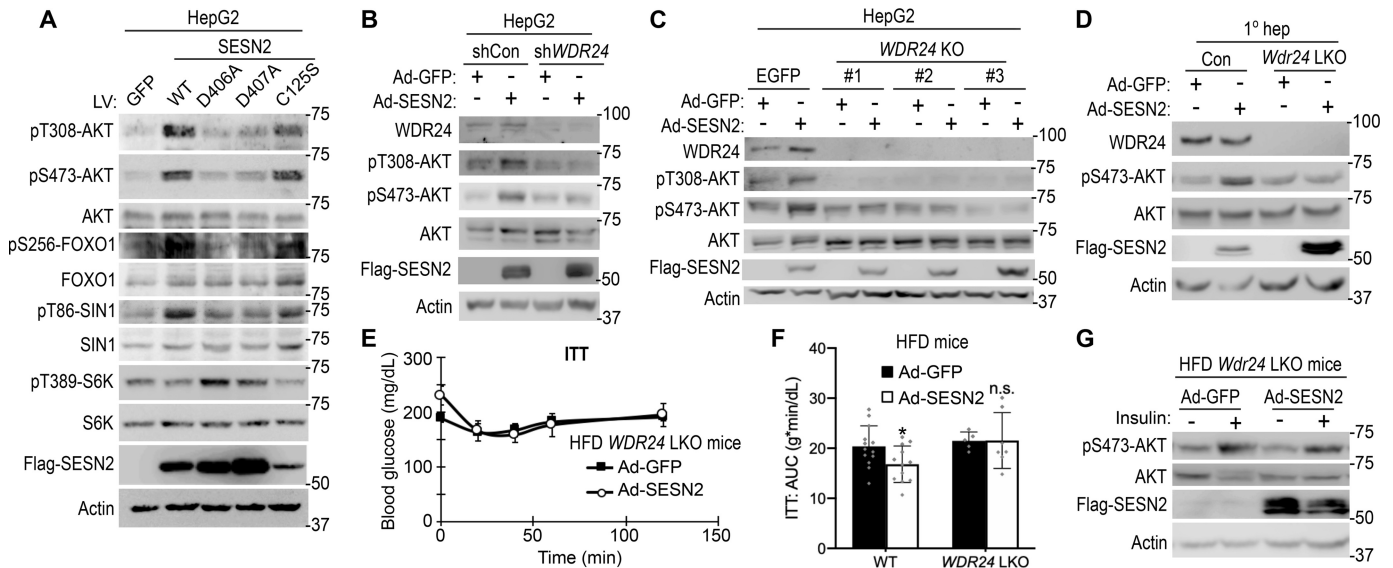
Figure 4. Sestrin2 requires GATOR2 to activate AKT. *A*, HepG2 cells were infected with lentiviruses (*LV*) that express control (*Con*, GFP), WT, or single-residue mutant forms of Sestrin2 (D406A, D407A, and C125S), serum-starved, and subjected to immunoblotting. *B*, HepG2 cells expressing control (pLKO-Con) or WDR24 (pLKO-WDR24) shRNA were treated with Ad-GFP or Ad-SESN2, serum-starved, and then subjected to immunoblotting. *C*, HepG2 cells were subjected to control (EGFP) or *WDR24* gene knockout targeting using CRISPR/Cas9. Cells with confirmed knockouts were then treated with Ad-GFP or Ad-SESN2, serum-starved, and then subjected to immunoblotting. *D*, primary hepatocytes were isolated from contol (*Wdr24^f/f*) or liver-specific *Wdr24*-knockout (*Wdr24* LKO; *Wdr24^f/f/Alb-Cre*) livers, treated with Ad-GFP or Ad-SESN2, serum-starved for 3 h, and then subjected to immunoblotting. *E–G*, 2-month-old *Wdr24* LKO mice were fed a HFD for 2 additional months and administered tail vein injections of Ad-GFP ($n = 5$) or Ad-SESN2 ($n = 7$). *E*, *Wdr24* LKO mice were subjected to an ITT 7 days after adenovirus administration. *F*, area under curve (*AUC*) was calculated for the ITT. The WT data are from Fig. 1*A*. *G*, livers were collected before (−) or 5 min after (+) an injection of insulin (0.8 unit/kg), and their lysates were analyzed by immunoblotting. The data are presented as means ± S.D. with individual data points (*bar graphs*) or means ± S.E. (*line graphs*). The *p* values were calculated between control (Ad-GFP) and Sestrin2-overexpressing (Ad-SESN2) groups from a two-tailed Student's *t* test: *n.s.*, not significant; *, $p < 0.05$.

serum-starved conditions (Fig. 3*D*). In contrast, both insulin and Sestrin2 had a strong positive effect on the catalytic activity of mTORC2 in phosphorylating AKT (Fig. 3*E*). Sestrin2-induced mTORC2 activation can lead to AKT Ser-473 phosphorylation, which can subsequently facilitate PDK1-mediated AKT T308 phosphorylation (33). Therefore, our data suggest that Sestrin2 acts through mTORC2 to activate AKT.

The GATOR2-binding function of Sestrin2 is required for AKT activation

We next investigated the biochemical basis of how Sestrin2 up-regulates mTORC2 and AKT. To address this problem, we utilized point mutants of Sestrin2 that specifically eliminate either its redox-regulating or GATOR2-binding functions (34). Like WT Sestrin2, Cys-125–mutated Sestrin2 with no oxidoreductase activity (5) strongly up-regulated mTORC2-dependent AKT phosphorylation, as well as AKT-dependent phosphorylation of its substrates FOXO1 and SIN1 (Fig. 4*A*). In contrast, Asp-406– and Asp-407–mutated Sestrin2, which cannot bind to the GATOR2 complex (5), was unable to up-regulate the AKT signaling pathway (Fig. 4*A*). These results suggest that the GATOR2-binding motif of Sestrin2, but not the redox-regulating motif, is critical for activating AKT.

GATOR2 is required for Sestrin2-induced AKT activation

WDR24 is a GATOR2 component that is essential for the Sestrin2-GATOR2 interaction (12). To directly assess the requirement of GATOR2 in Sestrin2-induced AKT activation, we ablated WDR24 function through both gene-silencing and knockout methods. In HepG2 cells, shRNA-mediated *WDR24*

silencing (Fig. 4*B*) and CRISPR/Cas9-mediated *WDR24* knockout (Fig. 4*C*) eliminated Sestrin2-induced AKT activation. Likewise, hepatocytes isolated from liver-specific *Wdr24*-knockout (*Wdr24* LKO) mice failed to increase AKT activation after Sestrin2 overexpression (Fig. 4*D*). Consistent with the requirement for WDR24 in Sestrin2-induced AKT activation, HFD-fed obese *Wdr24* LKO mice did not reduce blood glucose levels (Fig. 4, *E* and *F*) or increase hepatic AKT signaling (Fig. 4*G*) in response to Ad-SESN2 transduction, unlike HFD-fed obese WT mice (Figs. 1*A*, 2*A*, and 4*G*). Notably, *Wdr24* LKO mice retained insulin-induced AKT up-regulation (Fig. 4*G*), indicating that WDR24 is not required for insulin signaling to AKT but is required for Sestrin2-induced AKT activation. Taken together, these data indicate that Sestrin2 requires GATOR2 to activate AKT and improve metabolic phenotypes in HFD mice.

GATOR2 physically bridges Sestrin2 and mTORC2

To identify Sestrin2 targets in HepG2 cells, we performed proteomic analysis of Sestrin2-interacting proteins in HepG2 cells. Consistent with previous studies of the Sestrin2 interactome analyzed from MCF10A cells (12, 13) and HEK293T cells (11), the GATOR2 components appeared among the top Sestrin2 interacting proteins in HepG2 cells (Table S1). Based on the genetic requirement of GATOR2 in Sestrin2-induced AKT activation (Fig. 4), and the physical association between Sestrin2 and GATOR2 in HepG2 cells (Table S1), we hypothesized that GATOR2 may be the molecular conduit for Sestrin2-mediated up-regulation of mTORC2 and subsequent AKT activation. Recent reports showed that Sestrin2 physically associates
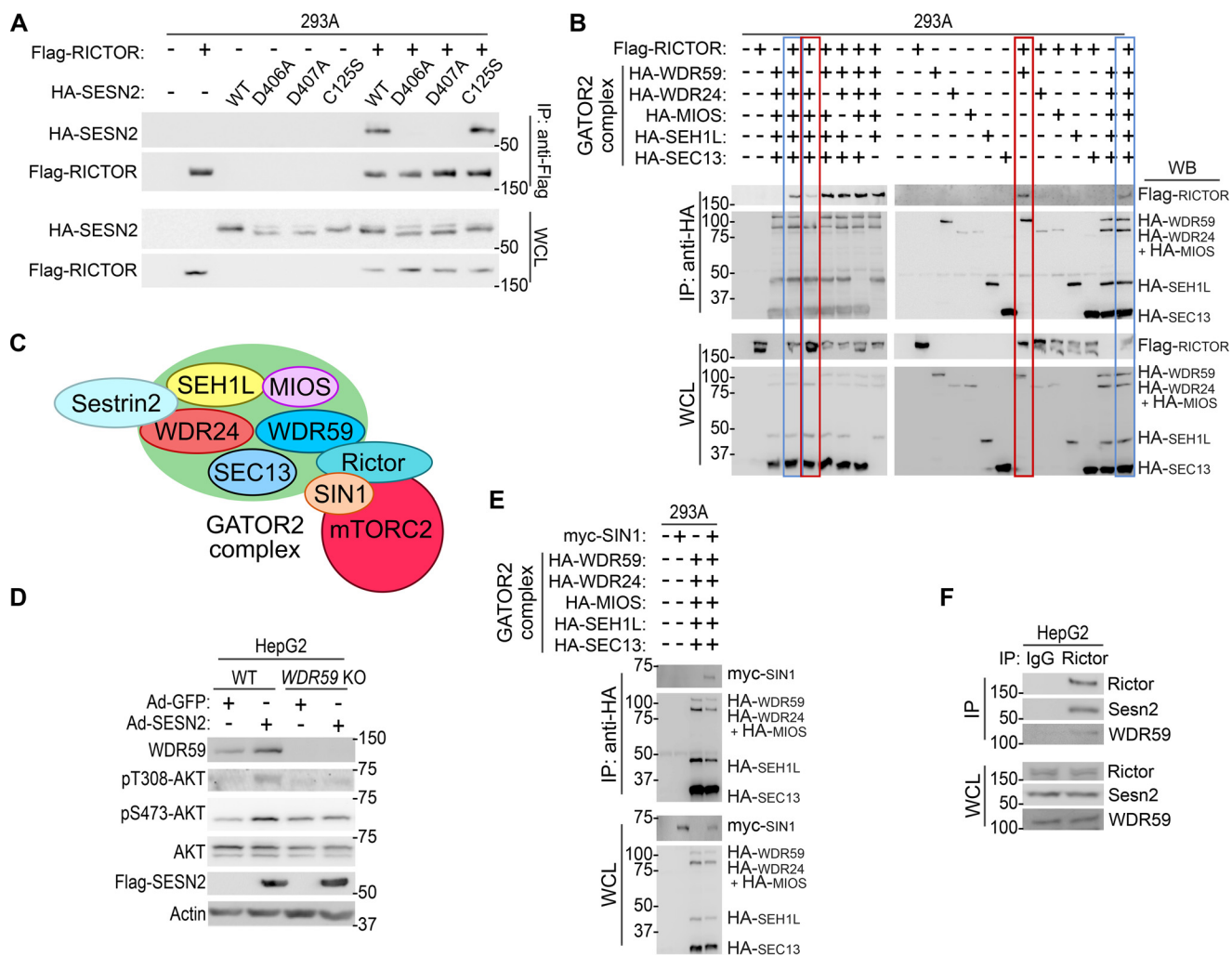
Figure 5. GATOR2 physically bridges Sestrin2 and mTORC2. *A* and *B*, HEK293 cells were transfected with the indicated constructs for 48 h and then subjected to co-immunoprecipitation (*IP*) with the indicated antibodies. Immunoprecipitation complexes and whole cell lysates (*WCL*) were examined through immunoblotting. *C*, schematic of how GATOR2 interacts with Sestrin2 and mTORC2. WDR24 was critical for the Sestrin2–GATOR2 interaction, whereas WDR59 was critical for the GATOR2–Rictor interaction. *D*, HepG2 cells stably expressing control (WT) or *WDR59*-targeting CRISPR/Cas9 constructs were infected with Ad-GFP or Ad-SESN2, serum-starved overnight, and then subjected to immunoblotting. *E*, HEK293 cells were transfected with the indicated constructs for 48 h and then subjected to immunoprecipitation with the indicated antibodies. Immunoprecipitation complexes and WCL were examined through immunoblotting. *F*, HepG2 cells were subjected to control or anti-Rictor immunoprecipitation overnight. Immunoprecipitation complexes and WCL were examined through immunoblotting of endogenous proteins. *WB*, Western blotting.

with mTORC2 (9, 23), and consistent with this, we were able to replicate the interaction between Sestrin2 and Rictor, an mTORC2-specific protein (Fig. 5A). Interestingly, however, Sestrin2 mutants that cannot bind GATOR2 (*e.g.* D406A and D407A) lost the ability to bind Rictor (Fig. 5A). In contrast, the Cys-125–mutated Sestrin2 fully retained Rictor binding, indicating that the redox-regulating function of Sestrin2 is not required for the Sestrin2–mTORC2 interaction.

These findings raised the possibility that GATOR2 bridges Sestrin2 and mTORC2. We therefore examined whether mTORC2 associates with GATOR2 through co-immunoprecipitation assays between Rictor and GATOR2 components. In addition to testing the interaction with the full complex, we systematically deleted subcomponents of GATOR2 or systematically expressed single components of GATOR2 to identify the GATOR2 subcomponent(s) that are responsible for the GATOR2–Rictor interaction. Interestingly, we found that GATOR2 and Rictor interact (Fig. 5B, *blue boxes*), and more-

over, the WDR59 subcomponent of GATOR2 was critical and sufficient for this interaction. When WDR59 was not expressed, the interaction between Rictor and GATOR2 was very weak (Fig. 5B, *red box* in *left panel*), and WDR59 alone pulled down Rictor (Fig. 5B, *red box* in *right panel*). Previous work showed that WDR24 is critical for the Sestrin2–GATOR2 interaction (12), and our current work identifies WDR59 as a critical component for the GATOR2–Rictor interaction (Fig. 5C). These data suggest that Sestrin2 and Rictor interact through GATOR2, containing both WDR24 and WDR59. Indeed, like WDR24, WDR59 was also required for Sestrin2-induced AKT activation; Sestrin2 failed to up-regulate AKT in *WDR59* KO HepG2 cells generated through CRISPR targeting (Fig. 5D). In addition, we confirmed the GATOR2–mTORC2 interaction by showing that Sin1, another critical mTORC2-specific subcomponent, also interacted with the full GATOR2 complex (Fig. 5E). Finally, we also observed Rictor–Sestrin2 and Rictor–WDR59 interactions at the
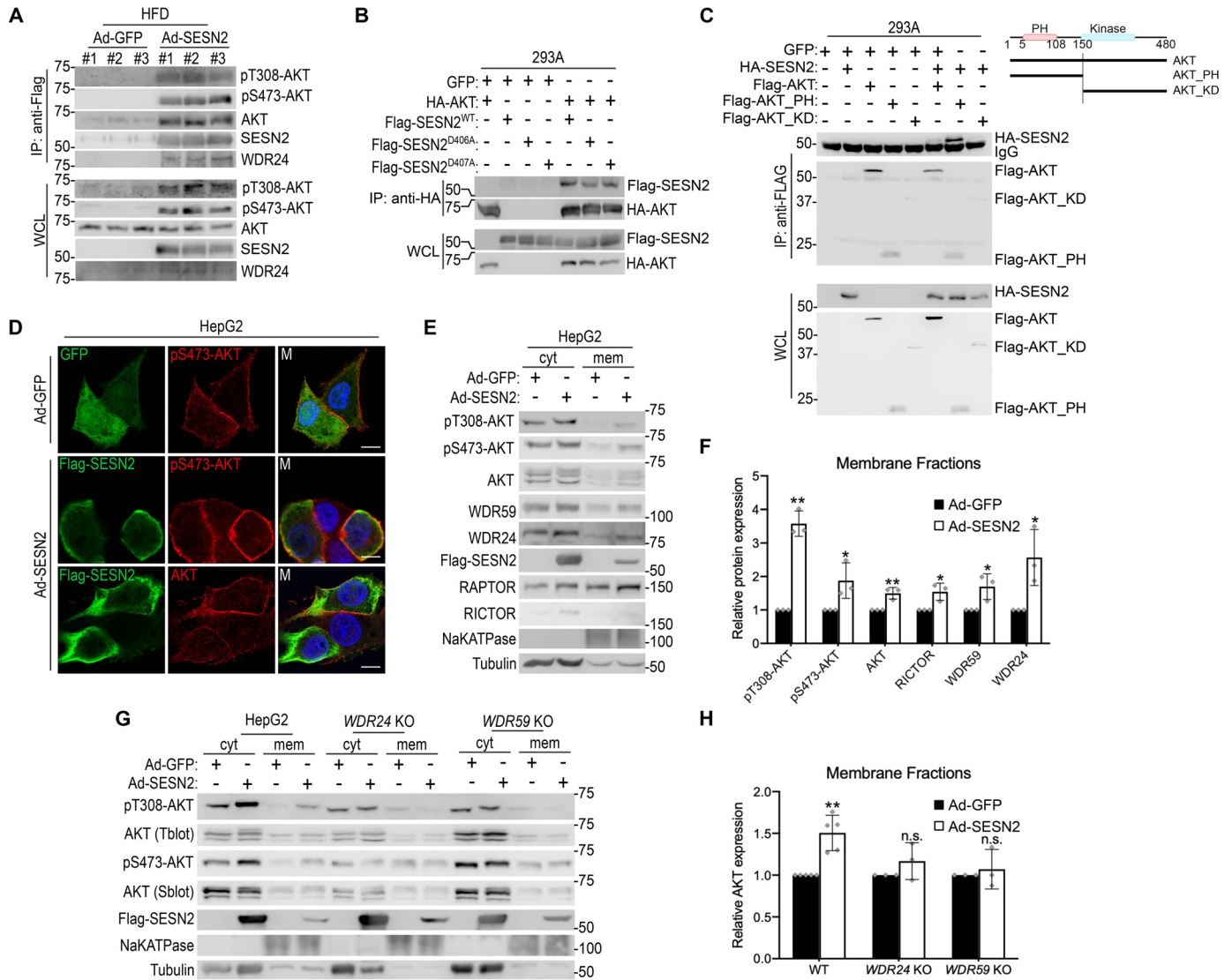
Figure 6. Sestrin2 induces AKT translocation to the plasma membrane. *A*, liver lysates from Ad-GFP– and Ad-SESN2–infected mice, described in the legend to Fig. 1, were subjected to anti-FLAG immunoprecipitation (*IP*). Immunoprecipitation complexes and whole cell lysates (*WCL*) were examined through immunoblotting. *B* and *C*, HEK293 cells were transfected with the indicated constructs for 24 h and then subjected to immunoprecipitation with the indicated antibodies. Immunoprecipitation complexes and WCL were examined through immunoblotting. *D*, HepG2 cells were infected with Ad-GFP or Ad-SESN2, serum-starved overnight, and then analyzed by immunocytochemistry using the indicated antibodies. *E–H*, HepG2 cells were infected with Ad-GFP or Ad-SESN2, serum-starved overnight, and then subjected to membrane fractionation experiments and subsequent immunoblotting. *F*, membrane fractions for the indicated proteins were quantified by densitometry (*n* = 3). *G*, *WDR24* and *WDR59* were targeted using CRISPR/Cas9 in HepG2 cells. The cells with confirmed knockouts were subjected to the indicated treatments, membrane fractionation, and then immunoblotting. *H*, relative AKT protein expression was quantified by densitometry for membrane fractions (*n* ≥ 3). The data are presented as means ± S.D. with individual data points. The *p* values were calculated between control (Ad-GFP) and Sestrin2-overexpressing (Ad-SESN2) membrane fractions from a two-tailed Student's *t* test: *, $p < 0.05$; **, $p < 0.01$. *cyt*, cytosol fraction; *mem*, membrane protein fraction.

endogenous level in HepG2 cells (Fig. 5F). These data collectively suggest that GATOR2 bridges Sestrin2 and mTORC2 to enable Sestrin2-mediated activation of mTORC2 and AKT (Fig. 5C).

Sestrin2 directly binds to the PH domain of AKT

While examining the physical interaction between Sestrin2 and other proteins, we serendipitously found that overexpressed FLAG-tagged Sestrin2 pulls down endogenous AKT in liver tissue (Fig. 6A). The Sestrin2-interacting AKT proteins were phosphorylated at both Thr-308 and Ser-473 (Fig. 6A), suggesting that these are active AKT proteins. The Sestrin2–AKT interaction was also observable in HEK293A cells (Fig.

6B); interestingly, Sestrin2 mutants that cannot bind GATOR2 were still able to interact with AKT (Fig. 6B). Therefore, it seems that the Sestrin2-AKT interaction is independent of the interactions we observed above for the Sestrin2–GATOR2–mTORC2 complexes.

To dissect the interaction between Sestrin2 and AKT further, we transfected Sestrin2 with three different forms of AKT: full-length, PH domain only (F-AKT_PH: residues 1–149), or kinase domain only (F-AKT_KD: residues 150–480) truncated forms (Fig. 6C). Using an immunoprecipitation assay, we confirmed that Sestrin2 physically interacted with full-length AKT. Sestrin2 also slightly interacted with AKT_KD, but we found the strongest association with AKT_PH, the truncated form of

AKT that includes the PH domain only (Fig. 6C). Therefore, independently of GATOR2 and mTORC2, Sestrin2 binds the AKT PH domain, a domain important for AKT translocation to the plasma membrane through binding 3′-phosphorylated phosphoinositide lipids generated by PI3K (20).

Sestrin2 induces AKT plasma membrane translocation through GATOR2

We were curious whether the interaction between Sestrin2 and the PH domain of AKT could alter the subcellular localization of AKT. In serum-starved HepG2 cells, Sestrin2 overexpression through adenoviral transduction induced strong AKT activation at the plasma membrane (Fig. 6D). Total AKT was also generally translocated to the plasma membrane in Sestrin2-overexpressing cells (Fig. 6D). The Sestrin2-induced membrane localization of AKT also occurred in cell fractionation experiments; Sestrin2 overexpression increased the presence of both p-AKT and AKT in total membrane fractions (Fig. 6, E and F). Interestingly, the GATOR2 components WDR24 and WDR59 were also targeted to the membrane fraction upon Sestrin2 overexpression (Fig. 6, E and F). Therefore, we tested whether Sestrin2-induced AKT membrane translocation required GATOR2. *WDR24* KO and *WDR59* KO HepG2 cells, in which GATOR2 function is compromised, did not target AKT to the membrane fraction in response to Sestrin2 overexpression (Fig. 6, G and H). Therefore, even though Sestrin2 binding to AKT may not require GATOR2, GATOR2 is required for Sestrin2-induced AKT activation and its translocation to the plasma membrane.

Discussion

Insulin resistance represents one of the most prominent phenotypes exhibited by Sestrin-deficient animals (28). *Sesn2*-knockout mice (7) and *Sesn3*-knockout mice (9, 35), as well as *dSesn*-null flies (7), are all prone to developing insulin resistance and subsequent dysregulation of blood glucose homeostasis. Hypoactivity of insulin receptor-AKT signaling is commonly observed in these models, whereas mTORC1 signaling was aberrantly activated through a mechanism independent of insulin signaling regulation. Because Sestrins down-regulate mTORC1, it was thought that mTORC1 inhibition was the major cause of AKT up-regulation (28). However, Sestrin-induced AKT activation was observed when mTORC1 components were silenced or ablated (9, 23), suggesting that Sestrins may regulate AKT independently of mTORC1. Consistent with these reports, we confirmed that Sestrin2-induced AKT activation did not require mTORC1. Instead, Sestrin2 activated AKT by up-regulating mTORC2, a kinase upstream of AKT. Therefore, our results indicate that Sestrin2 not only suppresses mTORC1 but concurrently activates mTORC2, a finding that aligns with other work indicating that tuberous sclerosis complex and AMPK inhibit mTORC1 but activate mTORC2 (32, 36, 37).

We also defined the molecular mechanism by which Sestrin2 up-regulates mTORC2. AMPK was recently shown to up-regulate mTORC2 activity and signaling independently of mTORC1/S6K1-mediated negative feedback through direct phosphorylation of mTORC2 subunits (32). Because Sestrin2

represents an established AMPK activator (3), it was possible that Sestrin2/AMPK signaling mediates Sestrin2-induced mTORC2 activation. However, we found that Sestrin2 activated mTORC2 and AKT similarly in WT and *Ampk*-null cells, indicating that Sestrin2-induced mTORC2 activation could occur independently of AMPK.

Utilizing mutational studies, we showed that Sestrin2's GATOR2-binding residues were required for its activation of mTORC2 and AKT. Consistent with former studies reporting a direct interaction between Sestrin2 and mTORC2 (9, 23), we found a physical association between Sestrin2 and Rictor, an mTORC2-specific subunit. However, Sestrin2 mutants that lost GATOR2 binding were not able to interact with Rictor. Subsequent experiments suggested that GATOR2 acted as a bridge between Sestrin2 and mTORC2; GATOR2 interacts with Sestrin2 through WDR24 (12) and with mTORC2 through WDR59. Indeed, Sestrin2 was unable to up-regulate mTORC2 and AKT in cells with genetic deletion of either WDR24 or WDR59. These experiments showed that GATOR2 mediates Sestrin2-induced activation of mTORC2 and AKT. Finally, our data suggested that Sestrin2 affects AKT subcellular localization. Through both immunocytochemistry and fractionation experiments, we found that Sestrin2 overexpression enriched both pAKT and AKT at the membrane. Because Sestrin2, WDR24/WDR59, and AKT are all enriched in the membrane fraction in conditions of Sesn2 overexpression, it is possible that Sesn2–GATOR2 complexes somehow physically direct AKT translocation. However, it is also possible that Ser-473 phosphorylation, which depends on GATOR2–mTORC2, somehow promotes membrane translocation and further activation of AKT. The exact mechanism of how Sesn2–GATOR2 induces membrane translocation and activation of AKT needs to be further clarified in future studies.

Importantly, the unique ability of Sestrin2 to inhibit mTORC1, activate AMPK, and activate mTORC2 makes it an ideal candidate for extending an organism's life and health span. Although the mTORC1 inhibitor rapamycin extended lifespan in multiple animal models (38), it also coincided with serious side effects such as insulin resistance caused by suppression of mTORC2 assembly and thus function (39). Although chronic mTORC1 up-regulation is detrimental and accelerates aging, mTORC2 activity is required to maintain metabolic homeostasis because it is essential for insulin-dependent signal transduction. Therefore, many aging researchers have searched for genetic and pharmacological agents that specifically inhibit mTORC1 while preserving mTORC2 activity (40). Sestrin2 or its chemical mimetics may be candidates for such agents.

In addition, unlike other pathways that activate AKT (*i.e.* insulin), Sestrin2-induced AKT activation did not concurrently activate mTORC1. AKT typically up-regulates mTORC1 through inhibitory phosphorylation of the mTORC1 inhibitors tuberous sclerosis complex 2 (41) and PRAS40 (42, 43). Therefore, although forced AKT activation in the liver through PTEN inactivation (44) or constitutively active AKT (myr-AKT) expression (45) up-regulated insulin signaling, it also detrimentally hyperactivated mTORC1, resulting in hepatomegaly and hepatic fat accumulation. Even though Sestrin2 activated AKT, it did not up-regulate mTORC1 because it has an independent

inhibitory function on mTORC1. Therefore, unlike other models of AKT activation, Sestrin2 reduced liver fat accumulation while up-regulating insulin signaling. Consistent with these functional outcomes, Sestrin2 inhibited mRNA expression of both gluconeogenic and lipogenic genes.

In summary, we show that Sestrin2 up-regulates the mTORC2/AKT pathway through a novel mechanism involving the GATOR2 complex. Further investigation into this signaling axis may reveal a novel mechanism for improving insulin signaling and normalizing metabolism during obesity and insulin resistance.

Experimental procedures

Mice and diets

The $Wdr24^{f/f}$ ($Wdr24^{tm1c}$)/Alb-Cre strain was generated from the $Wdr24^{tm1a(KOMP)Mbp}$ mouse line obtained from the University of California, Davis Mouse Biology program by breeding with the FLPo strain, backcrossed into the C57BL/6J background, and then crossed with the Alb-Cre line. 2-month-old WT or $Wdr24^{f/f}$/Alb-Cre mice of the C57BL/6J background were kept on a HFD (Bioserv S3282) for an additional 2 months. Insulin tolerance tests were performed on 25 WT mice and 12 $Wdr24^{f/f}$/Alb-Cre mice. In each cohort, littermate mice were divided into two groups and injected with adenoviruses through the tail vein. The insulin tolerance test (ITT) was performed at 4–10 days after adenoviral injection. For the ITT, the mice were fasted for 4–6 h in the morning and then injected with insulin (0.65 unit/kg body weight intraperitoneally). Blood glucose was measured 0, 20, 40, 60, and 120 min after insulin injection using a OneTouch Ultra glucose meter. At 10 days after adenoviral injection, livers were harvested under a surgical plane of isoflurane anesthesia before and after an injection of insulin (0.8 unit/kg) through the inferior vena cava. All mice were housed at the Unit for Laboratory Animal Medicine, and all procedures were approved by the Institutional Animal Care and Use Committee at the University of Michigan.

Oil Red O staining

Optimum cutting temperature compound–embedded frozen liver sections were air-dried and rinsed with 60% isopropanol, followed by staining with fresh 0.5% Oil Red solution for 15 min. After staining, the slides were rinsed with 60% isopropanol, washed with distilled water, mounted, and analyzed under a light microscope (Olympus). For quantification, 10 randomly chosen fields were used for each mouse liver.

Quantitative RT-PCR

Total RNA was extracted from tissues using TRIzol (Invitrogen), and cDNA was made using Moloney murine leukemia virus–reverse transcriptase (Thermo Fisher catalog no. 28025013) and random hexamers (Invitrogen). Quantitative PCR was performed in a real-time PCR detection system (Applied Biosystems) with iQ SYBR Green Supermix (Bio-Rad) and the primers listed in Table S2. Relative mRNA expression was calculated from the comparative threshold cycle (C_t) values normalized to β-actin and expressed as fold change over control values.

Antibodies and reagents

Sestrin2 (catalog no. 10795) is from Proteintech. pT308-Akt (catalog no. 4056), pS473-Akt (catalog no. 4060), Akt (catalog no. 4691), pT389-S6K (catalog no. 9234), pT172-AMPK (catalog no. 2535), AMPKα (catalog no. 2532), mTOR (catalog no. 2983), Rictor (catalog no. 2114), WDR59 (catalog no. 53385), pS256-FOXO1 (catalog no. 9461), FOXO1 (catalog no. 2880), pT86-Sin1 (catalog no. 14716), Sin1 (catalog no. 12860), NaKATPase (catalog no. 23565), and Raptor (catalog no. 2280) are from Cell Signaling Technology. MAPKAP-1 (catalog no. 393166), WDR24 (catalog no. 244614), p70S6 kinase α (catalog no. 8418), and Rictor (catalog no. 271081) are from Santa Cruz Biotechnology. FLAG (clone no. M2) is from Sigma. HA (clone no. 3F10) is from Roche. Actin (clone no. JLA20), His (clone no. P5A11), Tubulin (clone no. E7), and c-Myc (clone no. 9E10) are from Developmental Studies Hybridoma Bank. Chemical inhibitors used in this study include rapamycin (LC Labs), BYL719 (Selleck), PP242 (Chemdea), Torin1 (Adooq), and LY294002 (LC Labs).

Western blotting

Cells or tissues were lysed in cell lysis buffer (20 mM Tris-Cl, pH 7.5, 150 mM NaCl, 1 mM EDTA, 1 mM EGTA, 2.5 mM sodium pyrophosphate, 1 mM β-glycerophosphate, 1 mM Na_3VO_4, 1% Triton X-100 or 1% NP-40 or 0.3% Chaps) containing protease inhibitor mixture (Roche). After clarification by centrifugation, lysates were boiled in SDS sample buffer, separated by SDS-PAGE, transferred to polyvinylidene difluoride membranes, and probed with the indicated antibodies. Primary antibody dilution factors were 1:200 for Santa Cruz antibodies and 1:1000 for all others. After incubation with secondary antibodies conjugated with horseradish peroxidase at 1:2000, and chemiluminescence was detected using LAS4000 (GE) system. All protein loading was normalized to total protein concentration determined using Bio-Rad protein assay (Bio-Rad catalog no. 5000006). Protein expression in membrane fractions were normalized by the level of NaKATPase. Primary antibodies were incubated in Western blocking reagent (Sigma–Aldrich catalog no. 11921681001) for phospho-specific antibodies or 5% blotting grade blocker (Bio-Rad catalog no. 1706404) for all other antibodies.

Cell culture and transfection

All cells were maintained in Dulbecco's modified Eagle's medium (DMEM, Invitrogen) containing 10% fetal bovine serum (Sigma), 20 units/ml penicillin, and 50 mg/ml streptomycin. HepG2 is from ATCC. *WDR24*- and *WDR59*-knockout HepG2 cell lines were made from HepG2 using the Lenti-CRISPR v2 system (Addgene, originated from Feng Zhang's lab (46)) using the gRNA-encoding oligonucleotides: hWDR24 forward, CACCG TCA GGG TTG GCG CGC TCG AC; hWDR24 reverse, AAAC GTC GAG CGC GCC AAC CCT GA C; hWDR59 forward, CACCG ACC CGC GCA AAC GTC GGT AA; and hWDR59 reverse, AAAC TTA CCG ACG TTT GCG CGG GT C. After LentiCRISPR infection, multiple HepG2 cell clones with stable loss of targeted proteins were isolated through immunoblotting and used for the experiments. Primary hepatocytes were isolated from 2-month-old

control (*Wdr24^(f/f)*) and liver-specific *Wdr24*-knockout (*Alb-Cre/Wdr24^(f/f)*) mice as previously described (8). WT and *Ampkα1/2* KO MEFs were gifts from the Ken Inoki laboratory. Palmitic acid treatment was done as previously described (8, 47). HEK293A cells (Invitrogen) were transfected with plasmids expressing the indicated proteins using the polyethylenimine (Sigma) method as previously described (48). Sestrin constructs of WT and mutant forms are described in our previous work (5). GATOR2 constructs were originated from the David Sabatini lab (19) and obtained through Addgene. AKT and Rictor constructs were made by PCR amplification of corresponding cDNA and subsequent subcloning into pLU-CMV/FLAG or HA expression vectors. The Sin1 plasmid was a gift from the Do-Hyung Kim lab at the University of Minnesota.

Adenoviral and lentiviral production

Adenoviruses and lentiviruses were produced at the University of Michigan Vector Core. For adenoviral production, full-length human Sestrin2 coding sequence, attached to an N-terminal FLAG tag, was cloned into the pACCMV shuttle vector and incorporated into the adenoviral backbone at the Vector Core to generate Ad-SESN2. Ad-GFP was used as the control. For lentiviral production, pLU–CMV–SESN2 lentiviruses expressing WT and mutant Sestrin2 were formerly described (5). Lentiviruses expressing shRNA–Sestrin2 were also formerly described (8). Lentiviruses expressing shRNA–WDR24 were obtained from Sigma (The RNAi Consortium no. TRCN0000130142).

Immunoprecipitation

The cells were lysed in cell lysis buffer with 0.3% Chaps, clarified by centrifugation, and then incubated with FLAG bead (catalog no. A2220, Sigma), HA bead (catalog no. A2095, Sigma), mouse IgG–Sepharose bead conjugate (catalog no. 3420, Cell Signaling), or Rictor Sepharose bead conjugate (catalog no. 5379, Cell Signaling) on a rotisserie at 4 °C for 2 h or overnight. The immunocomplexes were washed six times with the lysis buffer, and the samples were boiled with SDS sample buffer for 5 min at 95 °C and analyzed by immunoblotting.

In vitro PI3K assay

The assay was performed as previously described (49). In brief, HepG2 cells were incubated with Ad-GFP or Ad-SESN2 for 48 h and replaced with serum-free DMEM. After 12 h, the cells were treated with water (control) or 100 nM insulin for 3 min and then harvested. The lysates were immunoprecipitated with p-Tyr antibodies (catalog no. 9411, Cell Signaling) conjugated to a protein G/A bead, subjected to a lipid kinase assay with $[\gamma\text{-}^{32}P]$ATP and phosphatidylinositol, and then subjected to TLC and autoradiography to visualize PI3P.

In vitro mTORC2 kinase assay

HepG2 cells were treated with Ad-GFP or Ad-SESN2 and serum-starved overnight. The lysates were immunoprecipitated with anti-Rictor antibodies conjugated to a protein G/A bead, subjected to a kinase assay with ATP and recombinant full-length inactive His-AKT substrate (Millipore catalog no.

14-279), and then analyzed by immunoblotting, as previously described (50).

Protein identification by LC–tandem MS

HepG2 cells were infected with Ad-GFP or Ad-SESN2 for 24 h. The lysates were then immunoprecipitated with anti-FLAG bead on a rotisserie at 4 °C for 2 h, washed seven times in cell lysis buffer (20 mM Tris, pH 7.6, 150 mM NaCl, 1 mM EDTA, 1 mM EGTA, 2.5 mM sodium pyrophosphate, 1 mM β-glycerophosphate, 1 mM Na_3VO_4, 0.3% Chaps), and then washed two times in PBS. The samples were sent to the University of Michigan Proteomics Resource Facility and subjected to the protein identification service plus 3-h LC-MS/MS analysis, according to their standardized procedure as described below.

The beads were resuspended in 50 μl of 0.1 M ammonium bicarbonate buffer (pH ~8). Cysteines were reduced by adding 50 μl of 10 mM DTT and incubating at 45 °C for 30 min. The samples were cooled to room temperature, and alkylation of cysteines was achieved by incubating with 65 mM 2-chloroacetamide, under darkness, for 30 min at room temperature. An overnight digestion with 1 μg of sequencing grade, modified trypsin was carried out at 37 °C with constant shaking in a Thermomixer. Digestion was stopped by acidification, and peptides were desalted using SepPak C18 cartridges, using the manufacturer's protocol (Waters). The samples were completely dried using a vacuum concentrator (Eppendorf). The resulting peptides were dissolved in 8 μl of 0.1% formic acid, 2% acetonitrile solution, and 2 μl of the peptide solution were resolved on a nano-capillary reverse phase column (Acclaim PepMap C18, 2 micron, 50 cm, Thermo Scientific), using a 0.1% formic acid, 2% acetonitrile (buffer A) and 0.1% formic acid, 95% acetonitrile (buffer B) gradient at 300 nl/min over a period of 180 min (2–22% buffer B in 110 min, 22–40% in 25 min, 40–90% in 5 min, followed by holding at 90% buffer B for 5 min and re-equilibration with buffer A for 25 min). Eluent was directly introduced into Orbitrap Fusion tribrid mass spectrometer (Thermo Scientific), using an EasySpray source. MS1 scans were acquired at 120 K resolution (automatic gain control target = 1×10^6; max ionization time = 50 ms). Data-dependent collision-induced dissociation MS/MS spectra were acquired using Top speed method (3 s), following each MS1 scan (normalized collision energy ~32%; automatic gain control target 1×10^5; max ionization time 45 ms).

Proteins were identified by searching the MS/MS data against the *Homo sapiens* database (UniProt; November 11, 2016 download with 42,054 entries) using Proteome Discoverer (version 2.1, Thermo Scientific). Search parameters included MS1 mass tolerance of 10 ppm and fragment tolerance of 0.2 Da; two missed cleavages were allowed; carbamidimethylation of cysteine was considered fixed modification; and oxidation of methionine and deamidation of asparagine and glutamine were considered as potential modifications. The false discovery rate was determined using Percolator, and proteins/peptides with a false discovery rate of ≤1% were retained for further analysis.

Immunocytochemistry

Ad-GFP– or Ad-SESN2–treated HepG2 were grown on coverslips overnight. After incubation with serum-free DMEM

overnight, the cells were fixed with 4% paraformaldehyde and permeabilized with 0.2% Triton X-100. The cells were incubated with 3% BSA and then with primary antibodies (1:1000) in PBS for 2 h. After washing, the cells were incubated with Alexa Fluor–conjugated secondary antibodies (1:1000) for 1 h, washed with PBS, counterstained with 4′,6′-diamino-2-phenylindole (Invitrogen), and mounted in Vectashield anti-fade mounting medium (H-1000). The images were captured under a Leica SP5X confocal microscope.

Cell fractionation

Cytosol and membrane protein fractions were isolated using the Mem-PER Plus membrane protein extraction kit (Thermo Scientific), according to the manufacturer's recommendations.

Statistical analyses

The results are presented as means ± S.D. with individual data points for bar graphs or means ± S.E. for line graphs. Significance between two groups was calculated using a two-tailed Student's *t* test.

References

1. Lee, J. H., Budanov, A. V., Park, E. J., Birse, R., Kim, T. E., Perkins, G. A., Ocorr, K., Ellisman, M. H., Bodmer, R., Bier, E., and Karin, M. (2010) Sestrin as a feedback inhibitor of TOR that prevents age-related pathologies. *Science* **327**, 1223–1228 CrossRef Medline
2. Yang, Y. L., Loh, K. S., Liou, B. Y., Chu, I. H., Kuo, C. J., Chen, H. D., and Chen, C. S. (2013) SESN-1 is a positive regulator of lifespan in *Caenorhabditis elegans*. *Exp. Gerontol.* **48**, 371–379 CrossRef Medline
3. Budanov, A. V., Lee, J. H., and Karin, M. (2010) Stressin' Sestrins take an aging fight. *EMBO Mol. Med.* **2**, 388–400 CrossRef Medline
4. Budanov, A. V., Sablina, A. A., Feinstein, E., Koonin, E. V., and Chumakov, P. M. (2004) Regeneration of peroxiredoxins by p53-regulated sestrins, homologs of bacterial AhpD. *Science* **304**, 596–600 CrossRef Medline
5. Kim, H., An, S., Ro, S. H., Teixeira, F., Park, G. J., Kim, C., Cho, C. S., Kim, J. S., Jakob, U., Lee, J. H., and Cho, U. S. (2015) Janus-faced Sestrin2 controls ROS and mTOR signalling through two separate functional domains. *Nat. Commun.* **6**, 10025 CrossRef Medline
6. Budanov, A. V., and Karin, M. (2008) p53 target genes sestrin1 and sestrin2 connect genotoxic stress and mTOR signaling. *Cell* **134**, 451–460 CrossRef Medline
7. Lee, J. H., Budanov, A. V., Talukdar, S., Park, E. J., Park, H. L., Park, H. W., Bandyopadhyay, G., Li, N., Aghajan, M., Jang, I., Wolfe, A. M., Perkins, G. A., Ellisman, M. H., Bier, E., Scadeng, M., *et al.* (2012) Maintenance of metabolic homeostasis by Sestrin2 and Sestrin3. *Cell Metab.* **16**, 311–321 CrossRef Medline
8. Park, H. W., Park, H., Ro, S. H., Jang, I., Semple, I. A., Kim, D. N., Kim, M., Nam, M., Zhang, D., Yin, L., and Lee, J. H. (2014) Hepatoprotective role of Sestrin2 against chronic ER stress. *Nat. Commun.* **5**, 4233 CrossRef Medline
9. Tao, R., Xiong, X., Liangpunsakul, S., and Dong, X. C. (2015) Sestrin 3 protein enhances hepatic insulin sensitivity by direct activation of the mTORC2-Akt signaling. *Diabetes* **64**, 1211–1223 CrossRef Medline
10. Saxton, R. A., Knockenhauer, K. E., Wolfson, R. L., Chantranupong, L., Pacold, M. E., Wang, T., Schwartz, T. U., and Sabatini, D. M. (2016) Structural basis for leucine sensing by the Sestrin2-mTORC1 pathway. *Science* **351**, 53–58 CrossRef Medline
11. Chantranupong, L., Wolfson, R. L., Orozco, J. M., Saxton, R. A., Scaria, S. M., Bar-Peled, L., Spooner, E., Isasa, M., Gygi, S. P., and Sabatini, D. M. (2014) The Sestrins interact with GATOR2 to negatively regulate the amino-acid-sensing pathway upstream of mTORC1. *Cell Rep* **9**, 1–8 CrossRef Medline
12. Parmigiani, A., Nourbakhsh, A., Ding, B., Wang, W., Kim, Y. C., Akopiants, K., Guan, K. L., Karin, M., and Budanov, A. V. (2014) Sestrins inhibit mTORC1 kinase activation through the GATOR complex. *Cell Rep.* **9**, 1281–1291 CrossRef Medline
13. Kim, J. S., Ro, S. H., Kim, M., Park, H. W., Semple, I. A., Park, H., Cho, U. S., Wang, W., Guan, K. L., Karin, M., and Lee, J. H. (2015) Sestrin2 inhibits mTORC1 through modulation of GATOR complexes. *Sci. Rep.* **5**, 9502 CrossRef Medline
14. Sanli, T., Linher-Melville, K., Tsakiridis, T., and Singh, G. (2012) Sestrin2 modulates AMPK subunit expression and its response to ionizing radiation in breast cancer cells. *PLoS One* **7**, e32035 CrossRef Medline
15. Eid, A. A., Lee, D. Y., Roman, L. J., Khazim, K., and Gorin, Y. (2013) Sestrin 2 and AMPK connect hyperglycemia to Nox4-dependent endothelial nitric oxide synthase uncoupling and matrix protein expression. *Mol. Cell. Biol.* **33**, 3439–3460 CrossRef Medline
16. Morrison, A., Chen, L., Wang, J., Zhang, M., Yang, H., Ma, Y., Budanov, A., Lee, J. H., Karin, M., and Li, J. (2015) Sestrin2 promotes LKB1-mediated AMPK activation in the ischemic heart. *FASEB J.* **29**, 408–417 CrossRef Medline
17. Deng, W., Cha, J., Yuan, J., Haraguchi, H., Bartos, A., Leishman, E., Viollet, B., Bradshaw, H. B., Hirota, Y., and Dey, S. K. (2016) p53 coordinates decidual sestrin 2/AMPK/mTORC1 signaling to govern parturition timing. *J. Clin. Invest.* **126**, 2941–2954 CrossRef Medline
18. Kim, M., and Lee, J. H. (2015) Identification of an AMPK phosphorylation site in *Drosophila* TSC2 (gigas) that regulate cell growth. *Int. J. Mol. Sci.* **16**, 7015–7026 CrossRef Medline
19. Bar-Peled, L., Chantranupong, L., Cherniack, A. D., Chen, W. W., Ottina, K. A., Grabiner, B. C., Spear, E. D., Carter, S. L., Meyerson, M., and Sabatini, D. M. (2013) A tumor suppressor complex with GAP activity for the Rag GTPases that signal amino acid sufficiency to mTORC1. *Science* **340**, 1100–1106 CrossRef Medline
20. Manning, B. D., and Toker, A. (2017) AKT/PKB signaling: navigating the network. *Cell* **169**, 381–405 CrossRef Medline
21. Zhao, B., Shah, P., Budanov, A. V., Qiang, L., Ming, M., Aplin, A., Sims, D. M., and He, Y. Y. (2014) Sestrin2 protein positively regulates AKT enzyme signaling and survival in human squamous cell carcinoma and melanoma cells. *J. Biol. Chem.* **289**, 35806–35814 CrossRef Medline
22. Ben-Sahra, I., Dirat, B., Laurent, K., Puissant, A., Auberger, P., Budanov, A., Tanti, J. F., and Bost, F. (2013) Sestrin2 integrates Akt and mTOR signaling to protect cells against energetic stress-induced death. *Cell Death Differ.* **20**, 611–619 CrossRef Medline
23. Byun, J. K., Choi, Y. K., Kim, J. H., Jeong, J. Y., Jeon, H. J., Kim, M. K., Hwang, I., Lee, S. Y., Lee, Y. M., Lee, I. K., and Park, K. G. (2017) A positive feedback loop between Sestrin2 and mTORC2 is required for the survival of glutamine-depleted lung cancer cells. *Cell Rep.* **20**, 586–599 CrossRef Medline
24. Dai, J., Huang, Q., Niu, K., Wang, B., Li, Y., Dai, C., Chen, Z., Tao, K., and Dai, J. (2018) Sestrin 2 confers primary resistance to sorafenib by simultaneously activating AKT and AMPK in hepatocellular carcinoma. *Cancer Med* **7**, 5691–5703 CrossRef Medline
25. Chen, C. C., Jeon, S. M., Bhaskar, P. T., Nogueira, V., Sundararajan, D., Tonic, I., Park, Y., and Hay, N. (2010) FoxOs inhibit mTORC1 and activate Akt by inducing the expression of Sestrin3 and Rictor. *Dev Cell* **18**, 592–604 CrossRef Medline
26. Kim, M., Sujkowski, A., Namkoong, S., Gu, B., Cobb, T., Kim, B., Kowalsky, A. H., Cho, C. S., Semple, I., Ro, S. H., Davis, C., Brooks, S. V., Karin, M.,

Wessells, R. J., and Lee, J. H. (2020) Sestrins are evolutionarily conserved mediators of exercise benefits. *Nat. Commun.*, **11,** 190 CrossRef Medline

27. Segalés, J., Perdiguero, E., Serrano, A. L., Sousa-Victor, P., Ortet, L., Jardi, M., Budanov, A. V., Garcia-Prat, L., Sandri, M., Thomson, D. M., Karin, M., Lee, J. H., and Muñoz-Cánoves, P. (2020) Sestrin prevents atrophy of disused and aging muscles by integrating anabolic and catabolic signals. *Nat. Commun.*, **11,** 189 CrossRef Medline

28. Lee, J. H., Budanov, A. V., and Karin, M. (2013) Sestrins orchestrate cellular metabolism to attenuate aging. *Cell Metab.* **18,** 792– 801 CrossRef Medline

29. Um, S. H., D'Alessio, D., and Thomas, G. (2006) Nutrient overload, insulin resistance, and ribosomal protein S6 kinase 1, S6K1. *Cell Metab.* **3,** 393– 402 CrossRef Medline

30. Kim, M. J., Bae, S. H., Ryu, J. C., Kwon, Y., Oh, J. H., Kwon, J., Moon, J. S., Kim, K., Miyawaki, A., Lee, M. G., Shin, J., Kim, Y. S., Kim, C. H., Ryter, S. W., Choi, A. M., *et al.* (2016) SESN2/sestrin2 suppresses sepsis by inducing mitophagy and inhibiting NLRP3 activation in macrophages. *Autophagy* **12,** 1272–1291 CrossRef Medline

31. Gao, D., Nong, S., Huang, X., Lu, Y., Zhao, H., Lin, Y., Man, Y., Wang, S., Yang, J., and Li, J. (2010) The effects of palmitate on hepatic insulin resistance are mediated by NADPH oxidase 3-derived reactive oxygen species through JNK and p38MAPK pathways. *J. Biol. Chem.* **285,** 29965–29973 CrossRef Medline

32. Kazyken, D., Magnuson, B., Bodur, C., Acosta-Jaquez, H. A., Zhang, D., Tong, X., Barnes, T. M., Steinl, G. K., Patterson, N. E., Altheim, C. H., Sharma, N., Inoki, K., Cartee, G. D., Bridges, D., Yin, L., *et al.* (2019) AMPK directly activates mTORC2 to promote cell survival during acute energetic stress. *Sci. Signal.* **12**

33. Sarbassov, D. D., Guertin, D. A., Ali, S. M., and Sabatini, D. M. (2005) Phosphorylation and regulation of Akt/PKB by the rictor-mTOR complex. *Science* **307,** 1098 –1101 CrossRef Medline

34. Ho, A., Cho, C. S., Namkoong, S., Cho, U. S., and Lee, J. H. (2016) Biochemical basis of sestrin physiological activities. *Trends Biochem. Sci.* **41,** 621– 632 CrossRef Medline

35. Huang, M., Kim, H. G., Zhong, X., Dong, C., Zhang, B., Fang, Z., Zhang, Y., Lu, X., Saxena, R., Liu, Y., Zhang, C., Liangpunsakul, S., and Dong, X. C. (2019) Sestrin 3 protects against diet-induced nonalcoholic steatohepatitis in mice via suppression of the TGFβ signal transduction. *Hepatology*, in press CrossRef Medline

36. Huang, J., and Manning, B. D. (2009) A complex interplay between Akt, TSC2 and the two mTOR complexes. *Biochem. Soc. Trans.* **37,** 217–222 CrossRef Medline

37. Huang, J., and Manning, B. D. (2008) The TSC1–TSC2 complex: a molecular switchboard controlling cell growth. *Biochem. J.* **412,** 179 –190 CrossRef Medline

38. Ehninger, D., Neff, F., and Xie, K. (2014) Longevity, aging and rapamycin. *Cell. Mol. Life Sci.* **71,** 4325– 4346 CrossRef Medline

39. Lamming, D. W., Ye, L., Katajisto, P., Goncalves, M. D., Saitoh, M., Stevens, D. M., Davis, J. G., Salmon, A. B., Richardson, A., Ahima, R. S., Guertin, D. A., Sabatini, D. M., and Baur, J. A. (2012) Rapamycin-induced insulin resistance is mediated by mTORC2 loss and uncoupled from longevity. *Science* **335,** 1638 –1643 CrossRef Medline

40. Kennedy, B. K., and Lamming, D. W. (2016) The mechanistic target of rapamycin: the grand conducTOR of metabolism and aging. *Cell Metab.* **23,** 990 –1003 CrossRef Medline

41. Inoki, K., Li, Y., Zhu, T., Wu, J., and Guan, K. L. (2002) TSC2 is phosphorylated and inhibited by Akt and suppresses mTOR signalling. *Nat Cell Biol.* **4,** 648 – 657 CrossRef Medline

42. Vander Haar, E., Lee, S. I., Bandhakavi, S., Griffin, T. J., and Kim, D. H. (2007) Insulin signalling to mTOR mediated by the Akt/PKB substrate PRAS40. *Nat. Cell Biol.* **9,** 316 –323 CrossRef Medline

43. Sancak, Y., Thoreen, C. C., Peterson, T. R., Lindquist, R. A., Kang, S. A., Spooner, E., Carr, S. A., and Sabatini, D. M. (2007) PRAS40 is an insulin-regulated inhibitor of the mTORC1 protein kinase. *Mol. Cell* **25,** 903–915 CrossRef Medline

44. Stiles, B., Wang, Y., Stahl, A., Bassilian, S., Lee, W. P., Kim, Y. J., Sherwin, R., Devaskar, S., Lesche, R., Magnuson, M. A., and Wu, H. (2004) Liver-specific deletion of negative regulator Pten results in fatty liver and insulin hypersensitivity [corrected]. *Proc. Natl. Acad. Sci. U.S.A.* **101,** 2082–2087 CrossRef Medline

45. Ono, H., Shimano, H., Katagiri, H., Yahagi, N., Sakoda, H., Onishi, Y., Anai, M., Ogihara, T., Fujishiro, M., Viana, A. Y., Fukushima, Y., Abe, M., Shojima, N., Kikuchi, M., Yamada, N., *et al.* (2003) Hepatic Akt activation induces marked hypoglycemia, hepatomegaly, and hypertriglyceridemia with sterol regulatory element binding protein involvement. *Diabetes* **52,** 2905–2913 CrossRef Medline

46. Ran, F. A., Hsu, P. D., Wright, J., Agarwala, V., Scott, D. A., and Zhang, F. (2013) Genome engineering using the CRISPR-Cas9 system. *Nat. Protoc.* **8,** 2281–2308 CrossRef Medline

47. Park, H. W., Park, H., Semple, I. A., Jang, I., Ro, S. H., Kim, M., Cazares, V. A., Stuenkel, E. L., Kim, J. J., Kim, J. S., and Lee, J. H. (2014) Pharmacological correction of obesity-induced autophagy arrest using calcium channel blockers. *Nat. Commun.* **5,** 4834 CrossRef Medline

48. Horbinski, C., Stachowiak, M. K., Higgins, D., and Finnegan, S. G. (2001) Polyethyleneimine-mediated transfection of cultured postmitotic neurons from rat sympathetic ganglia and adult human retina. *BMC Neurosci.* **2,** 2 CrossRef Medline

49. Wang, L. P., and Summers, S. A. (2003) Measuring insulin-stimulated phosphatidyl-inositol 3-kinase activity. *Methods Mol. Med.* **83,** 127–136 Medline

50. Huang, J. (2012) An *in vitro* assay for the kinase activity of mTOR complex 2. *Methods Mol. Biol.* **821,** 75– 86 CrossRef Medline

ASBMB